Supplementary Information (SI) for Physical Chemistry Chemical Physics.

Supporting Information

Synthesis and physico-chemical study of new fluorescent *N*-naphthimidazole phosphoramidate oligonucleotides

Alina I. Novgorodtseva[a], Aleksey Y. Vorob'ev [b], Igor R. Filippov [b], Victor M. Golyshev[a], Anton A. Berdugin[a], Ivan I. Yushin[a], Svetlana V. Vasilyeva[†a] and Alexander A. Lomzov*[a]

[a]Institute of Chemical Biology & Fundamental Medicine, SB RAS, 8 Akad. Lavrentiev Avenue, Novosibirsk 630090, Russia

[b]N.N. Vorozhtsov Novosibirsk Institute of Organic Chemistry, SB RAS, 9 Akad. Lavrentiev Avenue, Novosibirsk 630090, Russia

[*] E-mail: lomzov@1bio.ru

[†] E-mail: svetlana2001@gmail.com

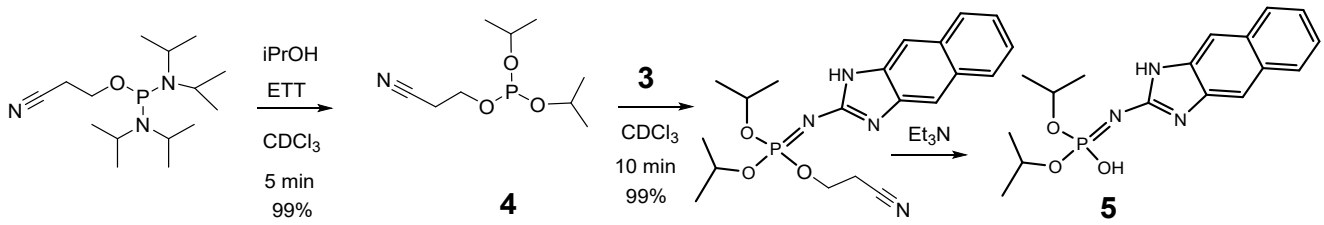

Scheme S1. Synthesis of diisopropyl(1H-naphtho[2,3-d]imidazol-2-yl)phosphorimidate 5.

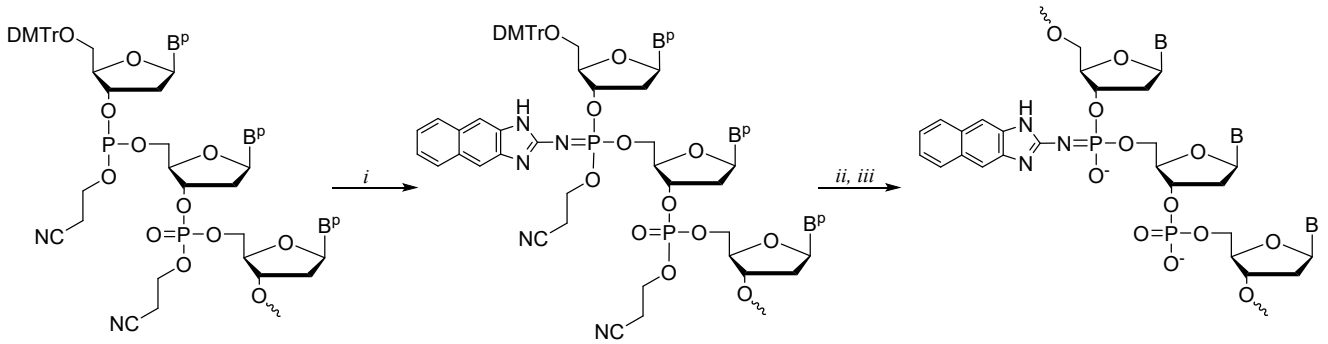

Scheme S2. Synthesis of oligodeoxyribonucleotides containing P*N*-naphthimidazole group(s) via the Staudinger reaction using 2-azido-naphthimidazole: (i) 0.5 M 3, DMSO, 30 °C, 45 min, (ii) automated DNA synthesis, and (iii) concentrated aqueous NH3, 55 °C, 8 h. B is a nitrogenous base and p is an N-protecting group.

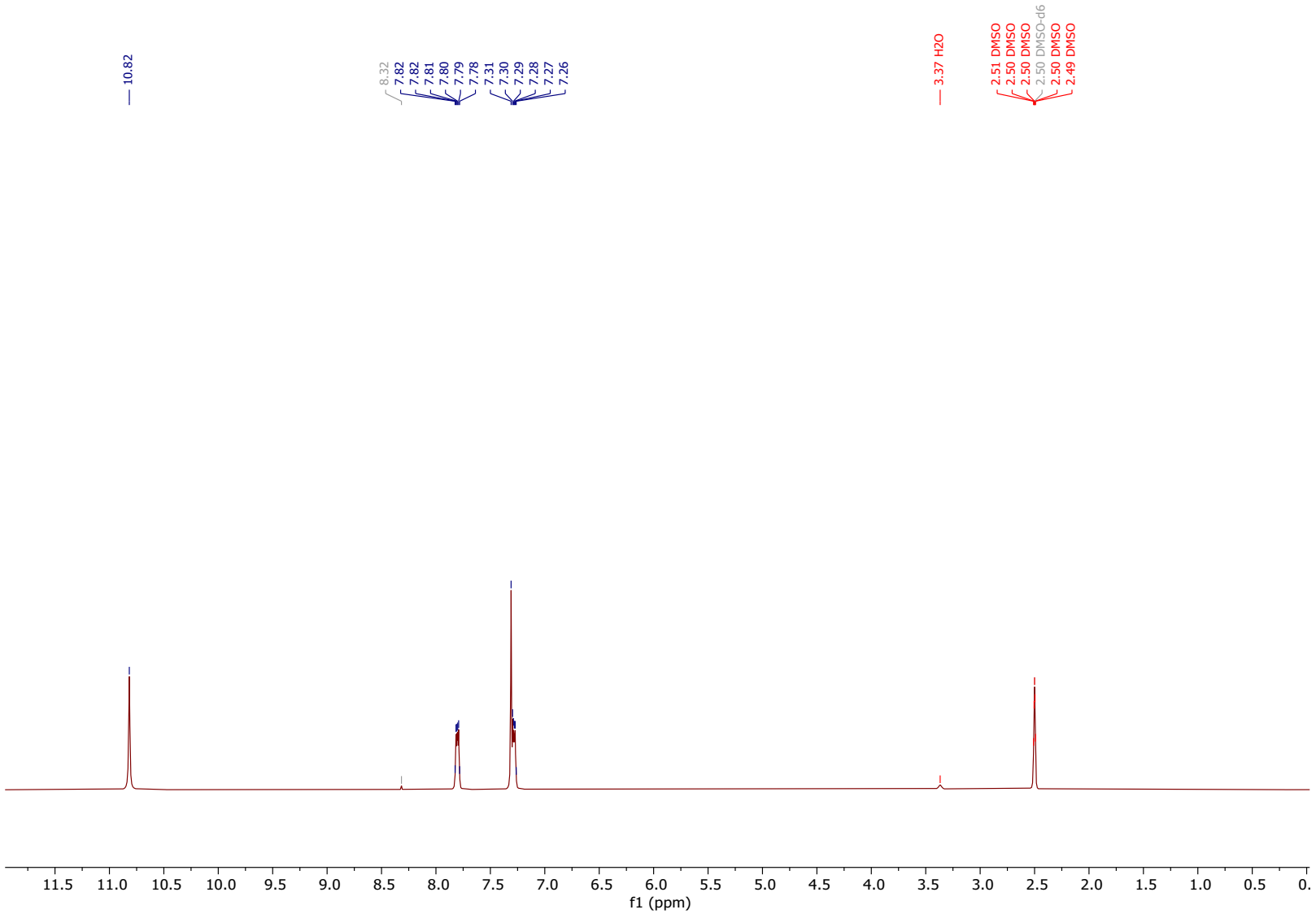

Figure S1. ^{1}H NMR spectrum of compound **1** (Scheme 2). Signal at 8.32 ppm corresponds to $CHCl_3$.

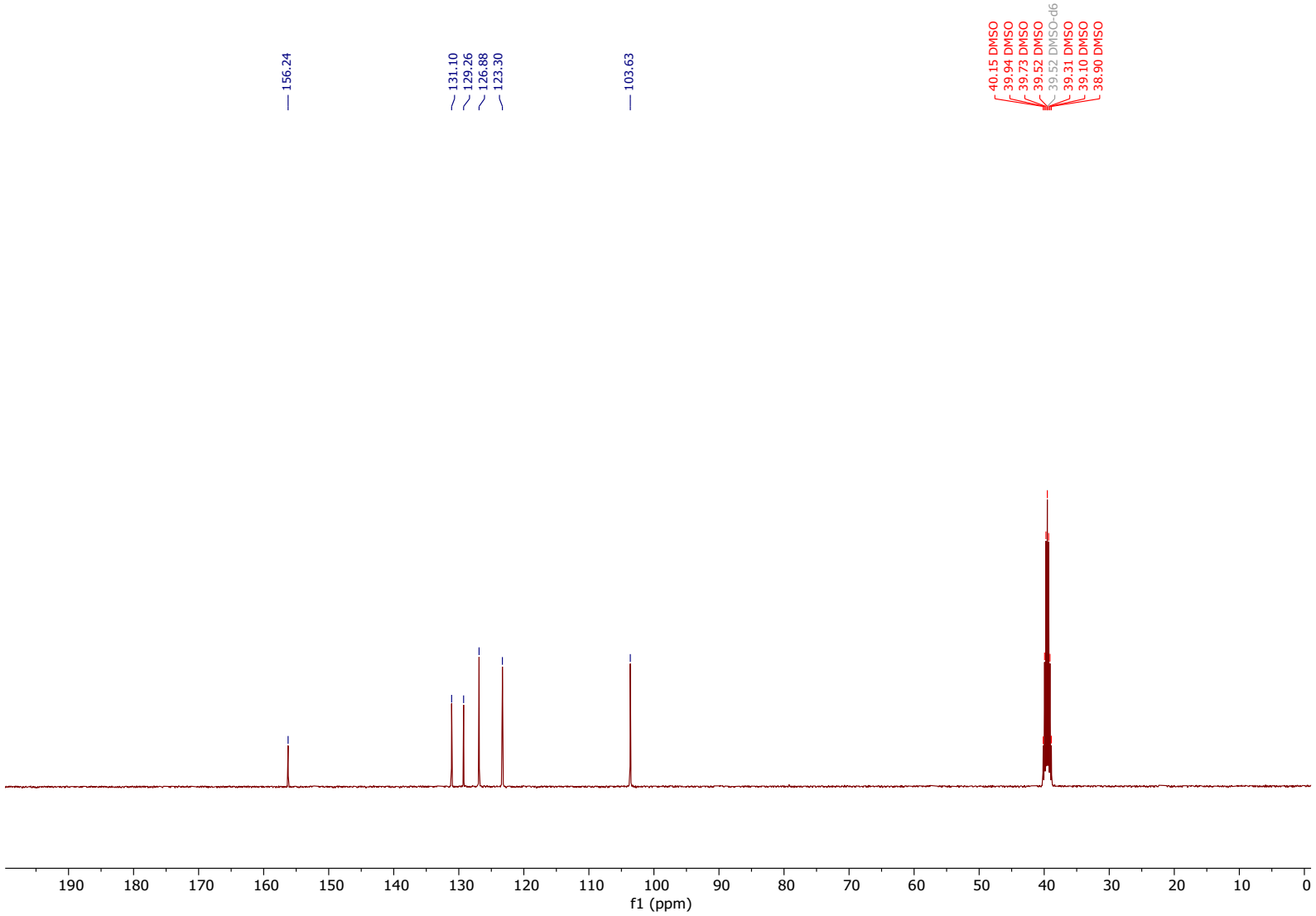

Figure S2. ^{13}C NMR spectrum of compound **1** (Scheme 2).

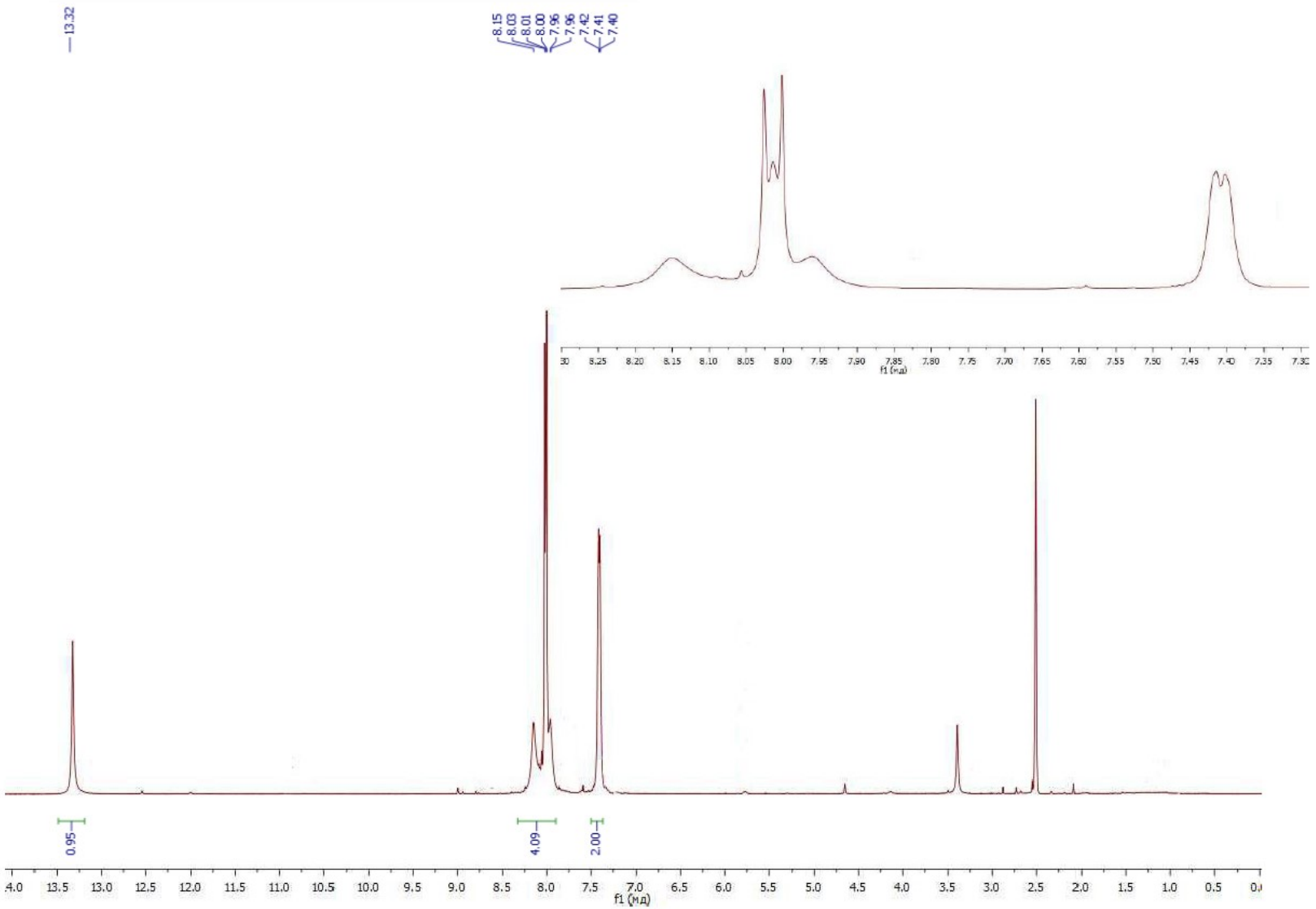

Figure S3. ^{1}H NMR spectrum of compound **2** (Scheme 2).

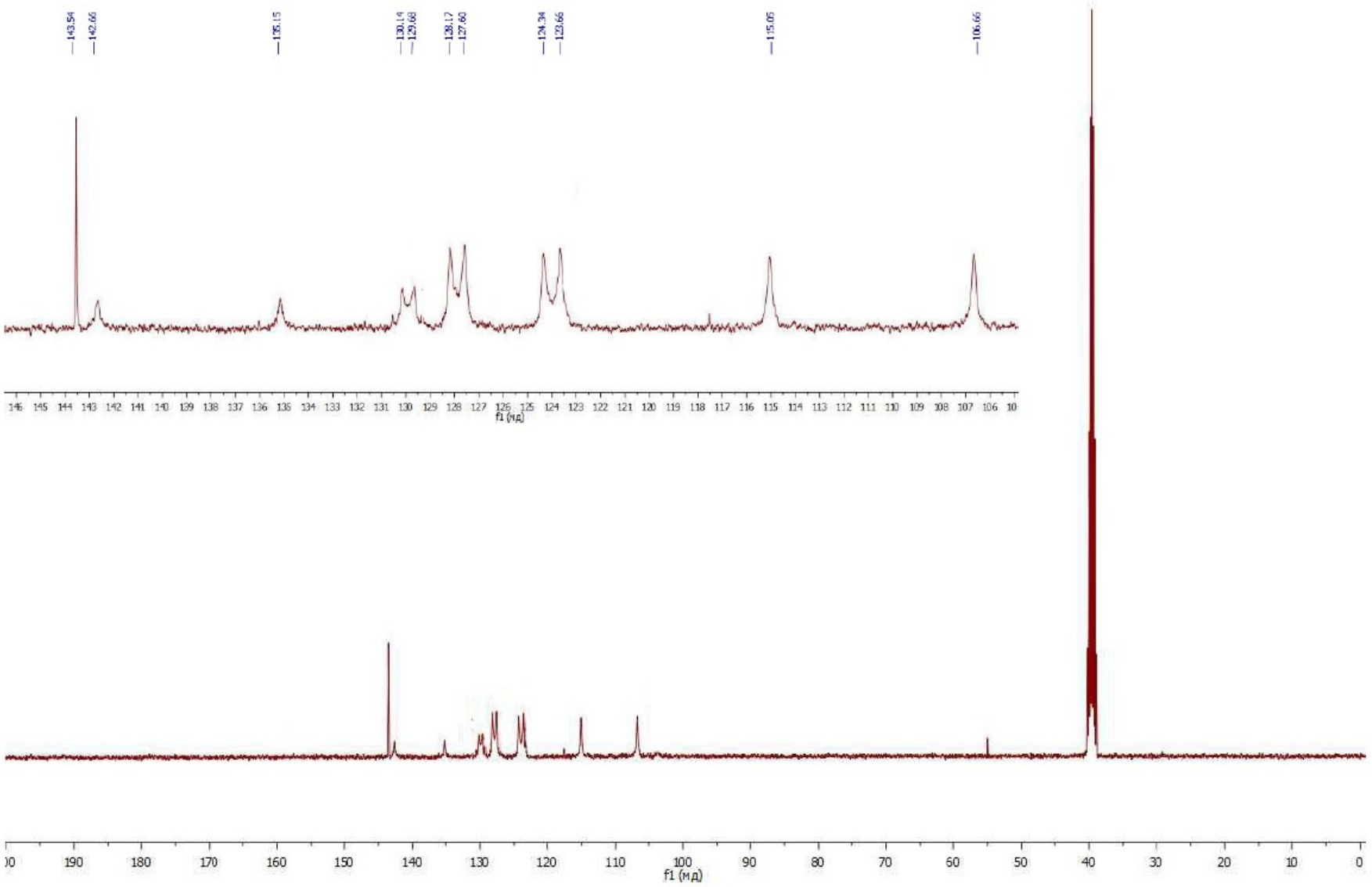

Figure S4. . ^{13}C NMR spectrum of compound **2** (Scheme 2).

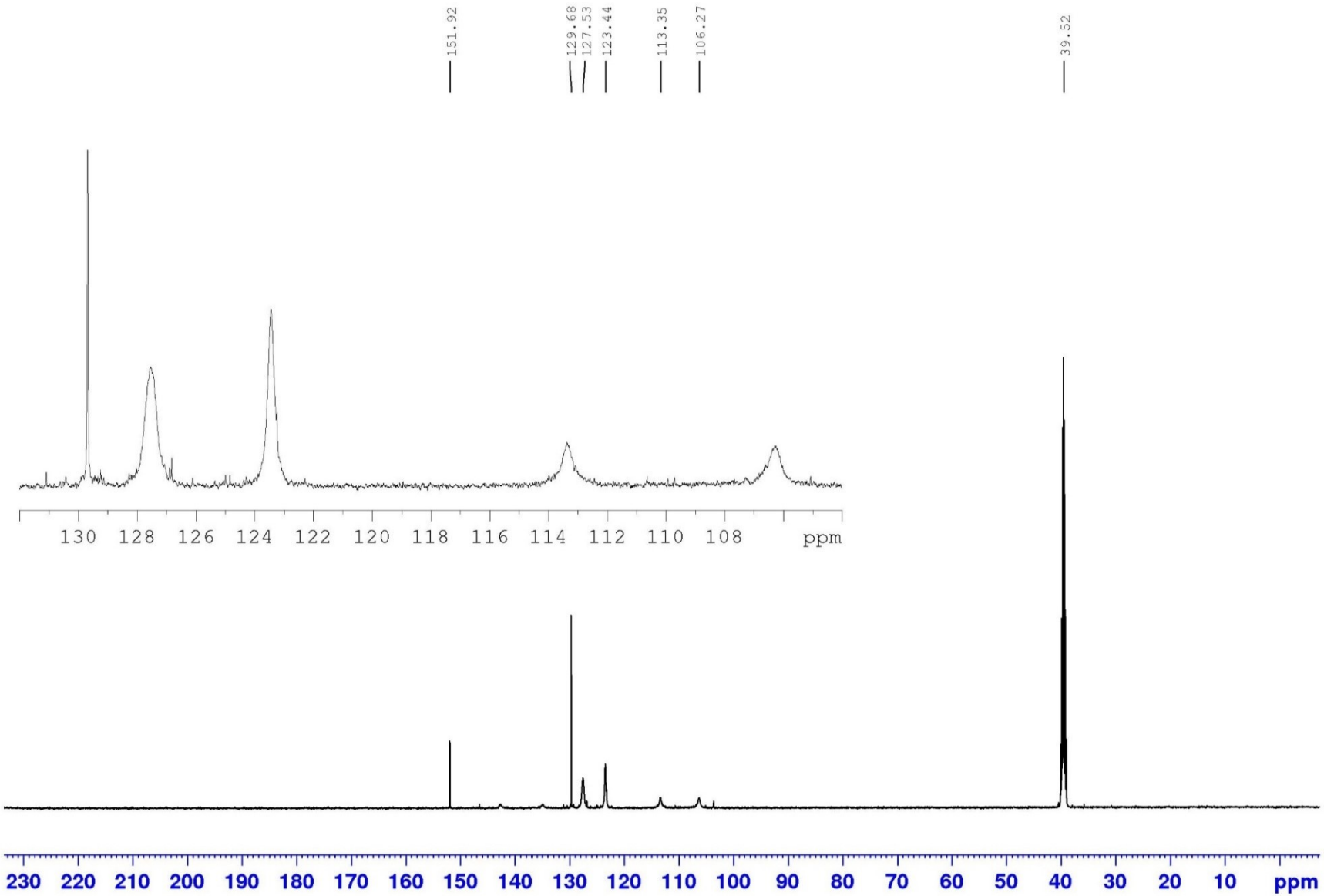

Figure S5. ^{13}C NMR (125.7 MHz, DMSO-d6) spectrum of 2-azido-1H-naphtho[2,3-d]imidazole **3** (Scheme 2).

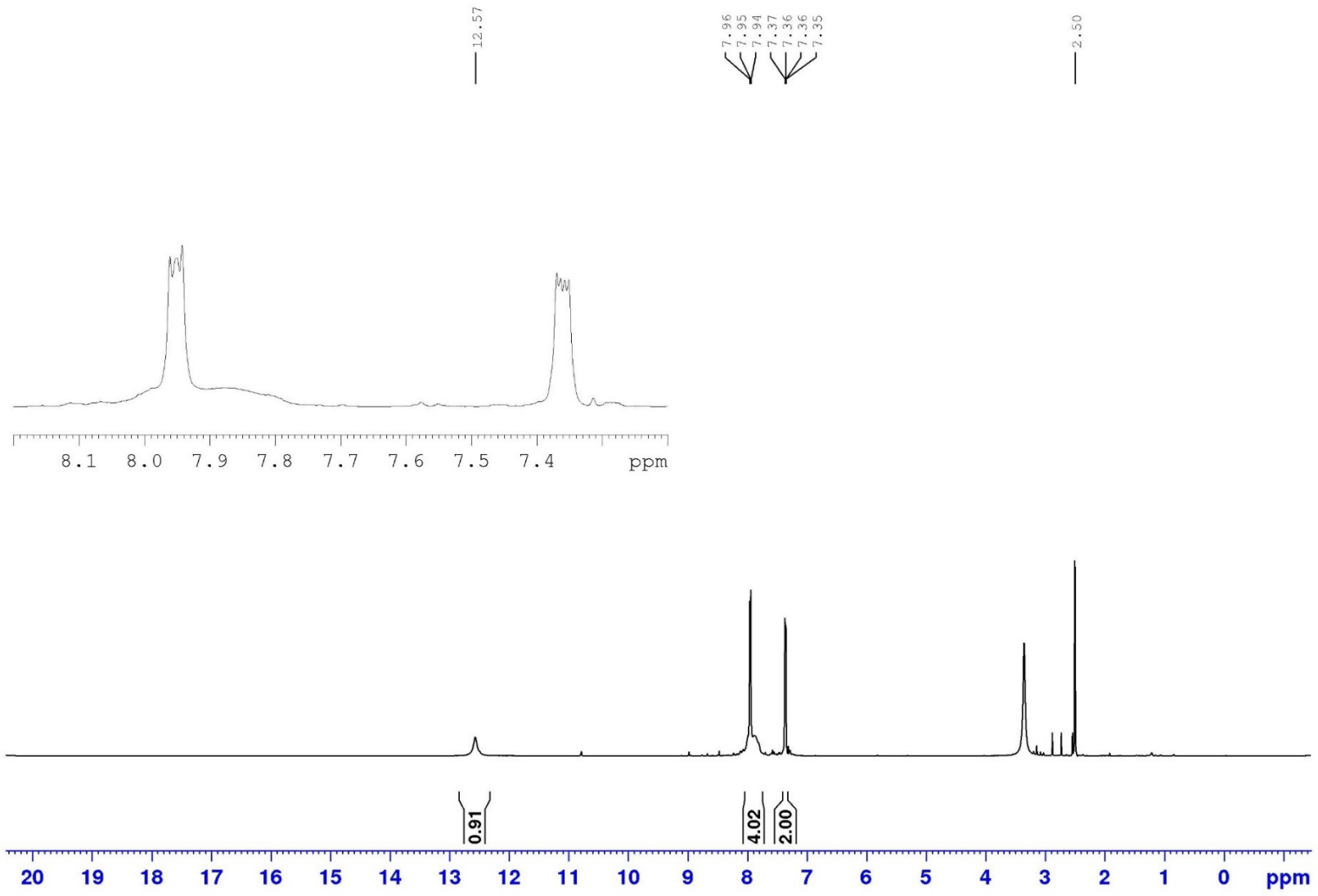

Figure S6. ^{1}H NMR (300 MHz, DMSO-d6) spectrum of 2-azido-1H-naphtho[2,3-d]imidazole **3** (Scheme 2).

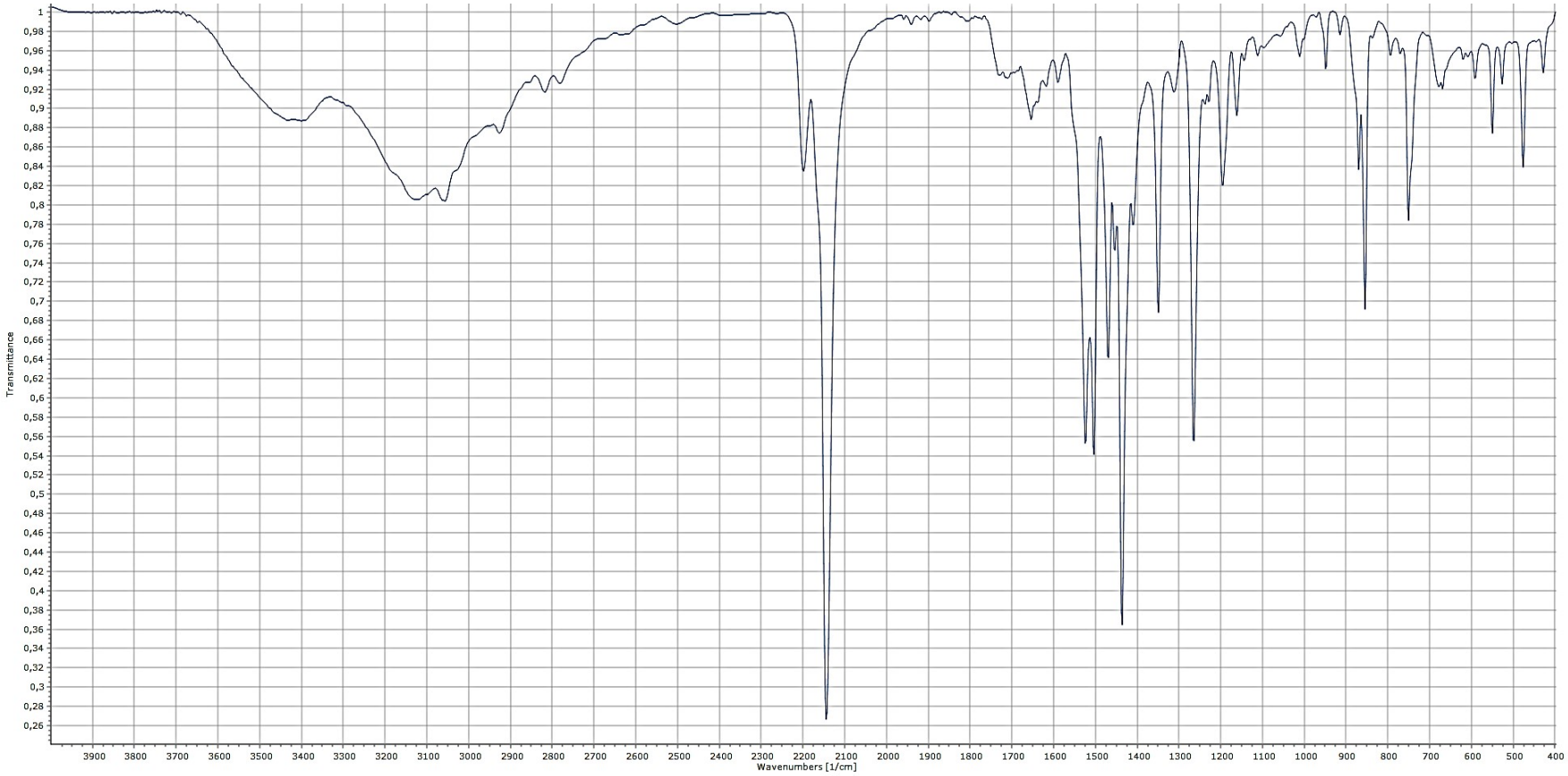

Figure S7. IR (KBr) spectrum of 2-azido-1H-naphtho[2,3-d]imidazole **3** (Scheme 2).

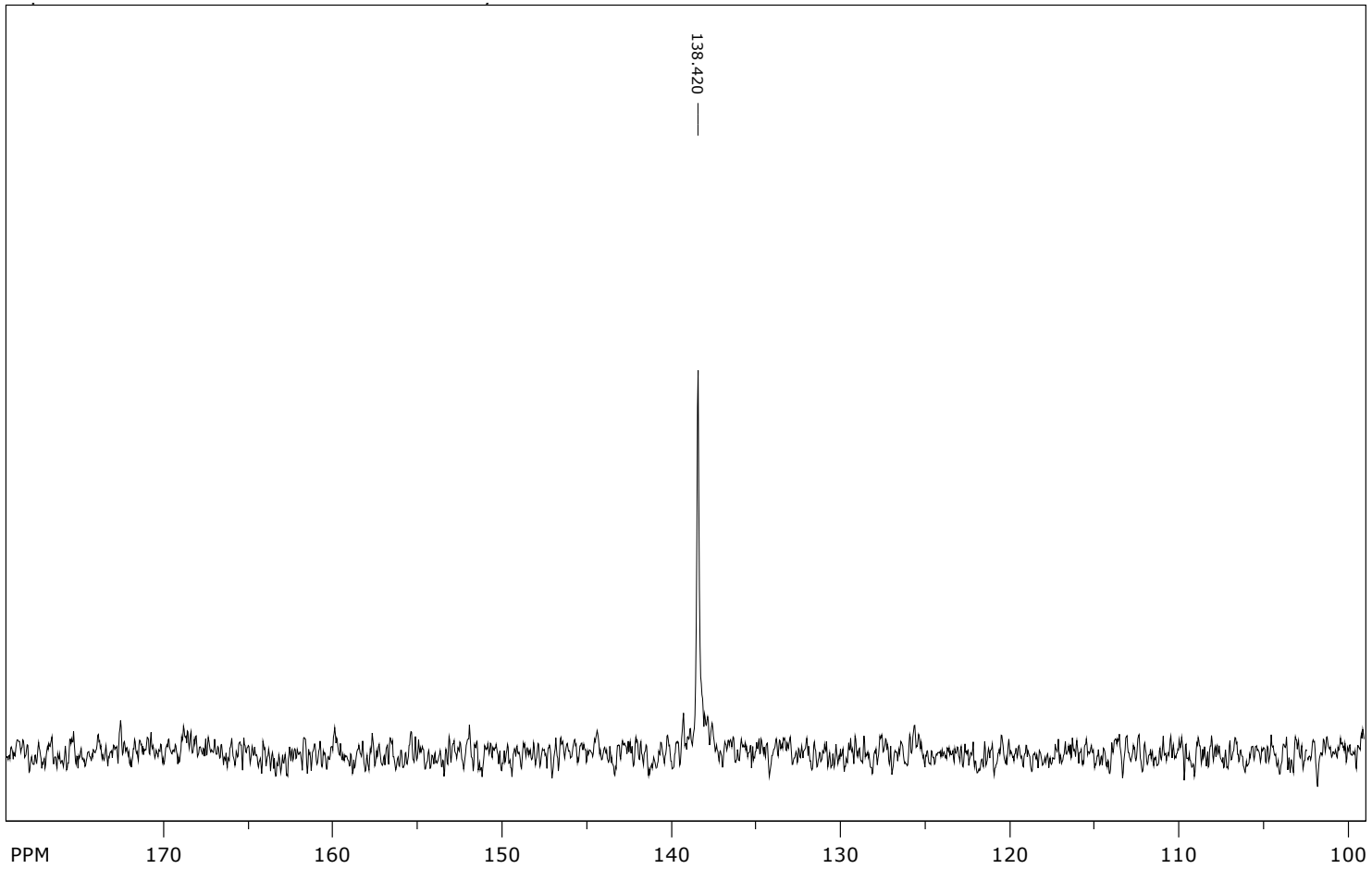

Figure S8. ^{31}P NMR (32.48 MHz, $CDCl_3$) spectrum of phosphitetriester **4** (Scheme S1).

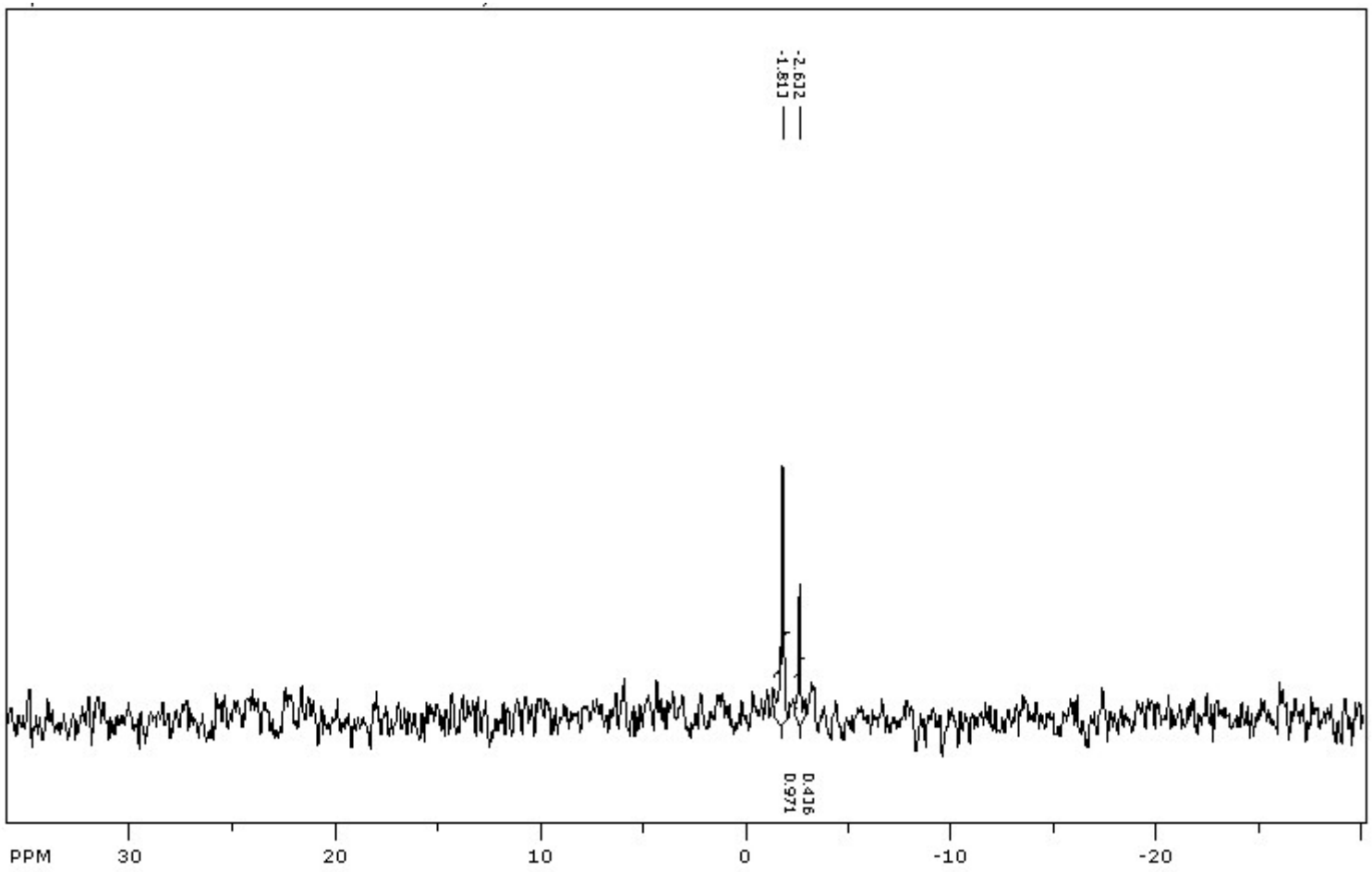

Figure S9. ^{31}P NMR (32.48 MHz, $CDCl_3$) spectrum of 2-cyanoethyl-diisopropyl(1H-naphtho[2,3-d]imidazol-2-yl)phosphorimidate intermediate product (Scheme S1). The formation of this product could occur in the presence of water, from the literature it is known that the signal -2.67 corresponds to the signal of unmodified 2-cyanoethyl diisopropylamidophosphate [Xiao-Lan C. et al. Study on the reaction of salicylic acid with dialkyl phosphite by NMR and electrospray ionization mass spectrometry //Chinese Journal of Chemistry. – 2005. – Т. 23. – №. 6. – С. 733-739].

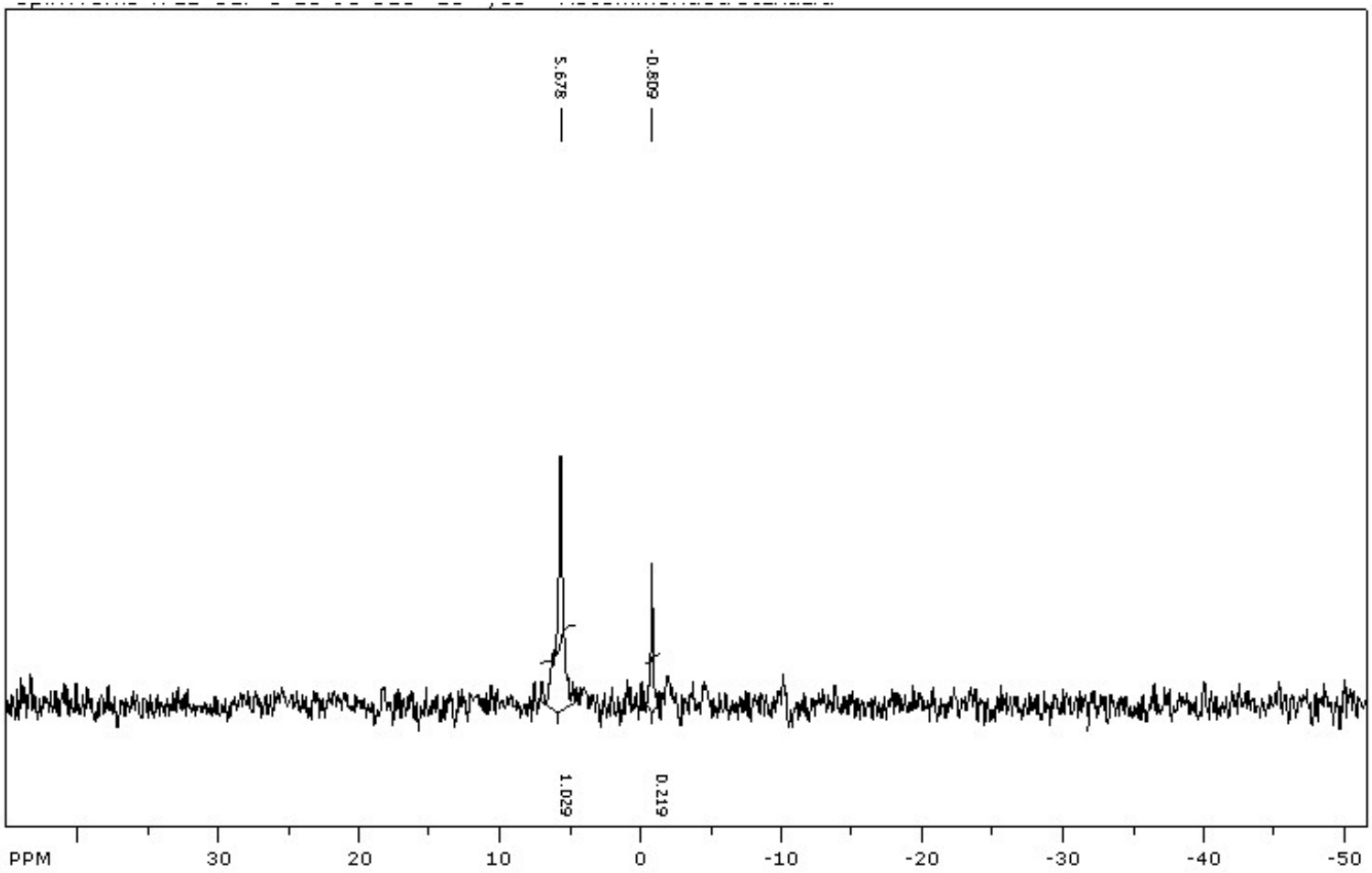

Figure S10. ^{31}P NMR (32.48 MHz, DMSO-d6) spectrum of compound **5** (Scheme S1).

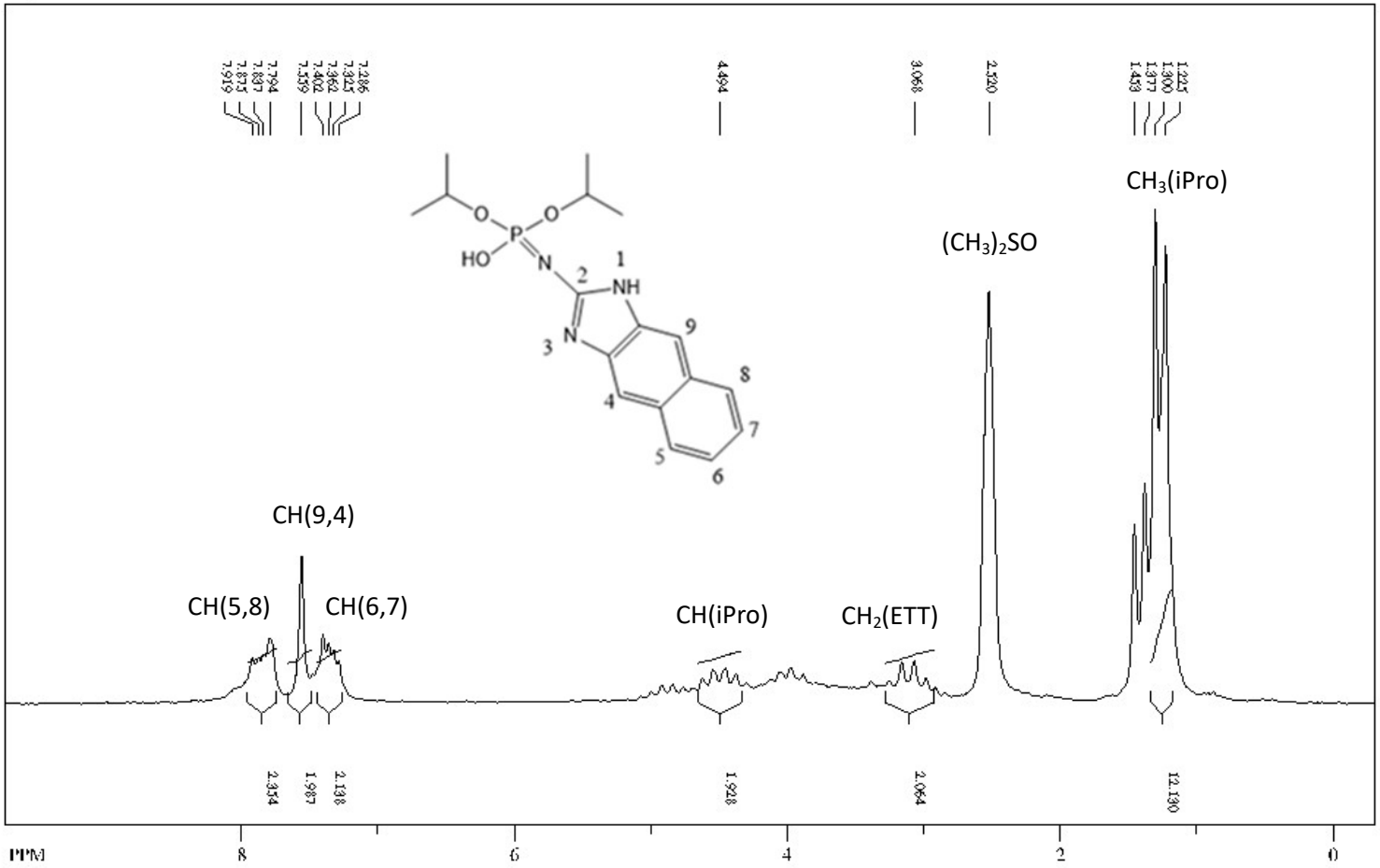

Figure S11. ^{1}H NMR (80 MHz, DMSO-d6) spectrum of compound **5** (Scheme S1). Additional signals are 3.14 ppm (m, 2H-CH_2(ETT)), 1.48 ppm (t, 3H-CH_3(ETT)) from ethylthiotetrazole impurity, and 2.54 ppm (s, 6H-DMSO).

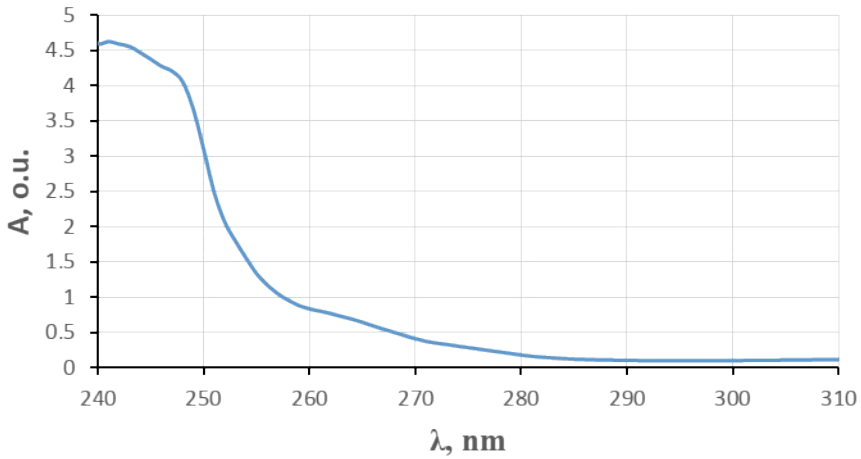

Figure S12. UV spectra of 2-azido-1H-naphtho[2,3-d]imidazole **3** (Scheme 2), (C=10-4 M in DMSO). λ 260: D=0.838 (ε(260) = 8380 l/mol/cm).

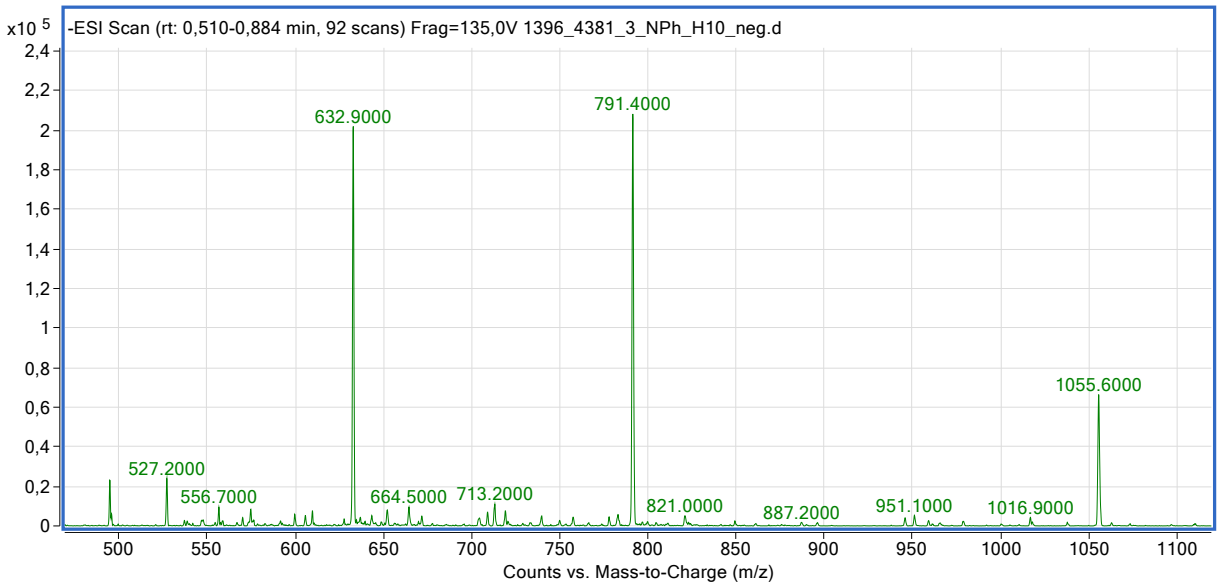

Figure S13. Mass spectrum (ESI LC-MS/MS in negative mode) of 5′-GCGCCAAAC^{NPh}A-3′ (3′-NPh-H10, Table 1).

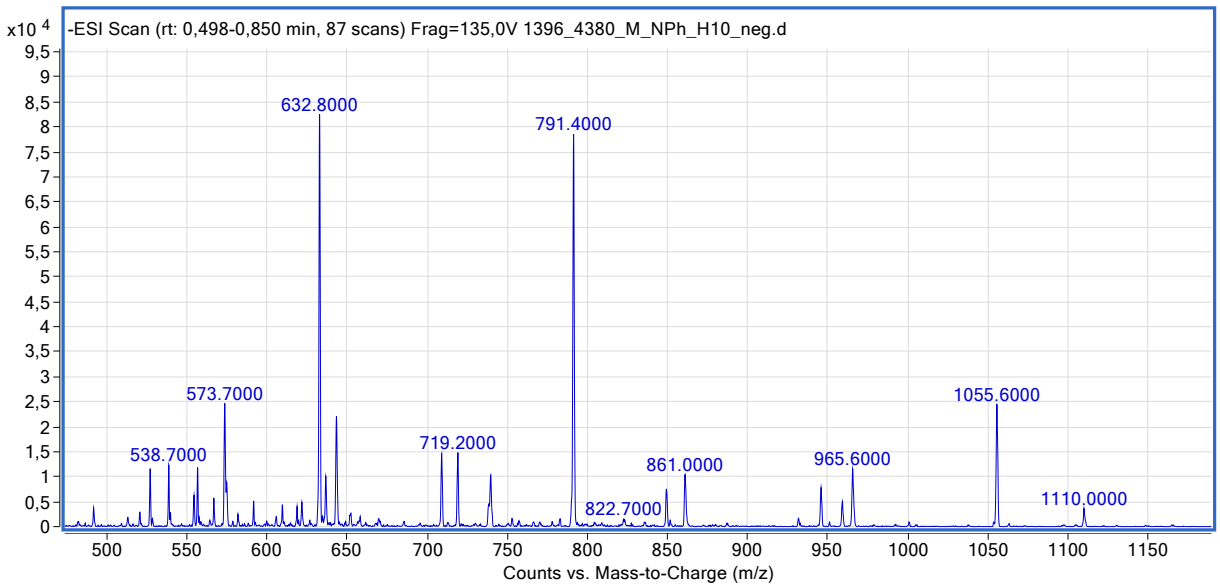

Figure S14. Mass spectrum (ESI LC-MS/MS in negative mode) of 5'-GCGCC^{NPh}AAACA-3' (M-NPh-H10, Table 1).

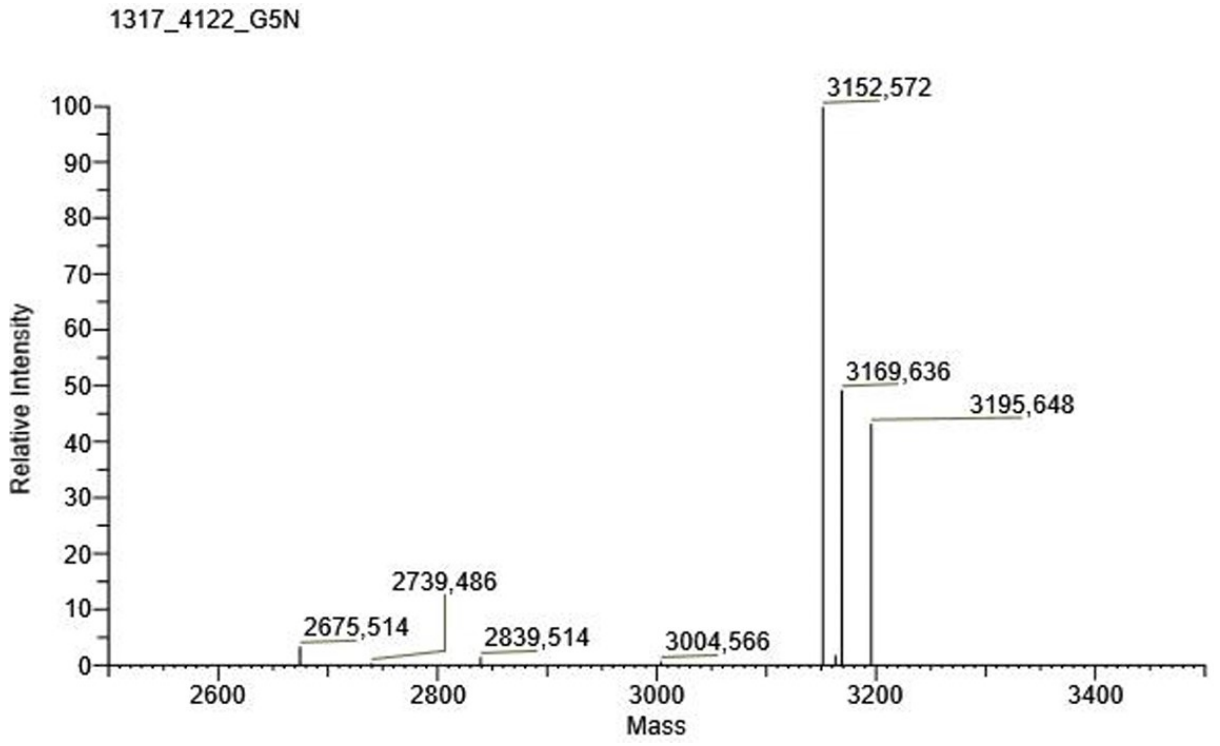

Figure S15. Mass spectrum (MALDI-TOF mass spectroscopy in negative mode) of reaction mixture of 5'-G^{NPh}CGCCAAACA-3' (5'-NPh-H10, Table 1).

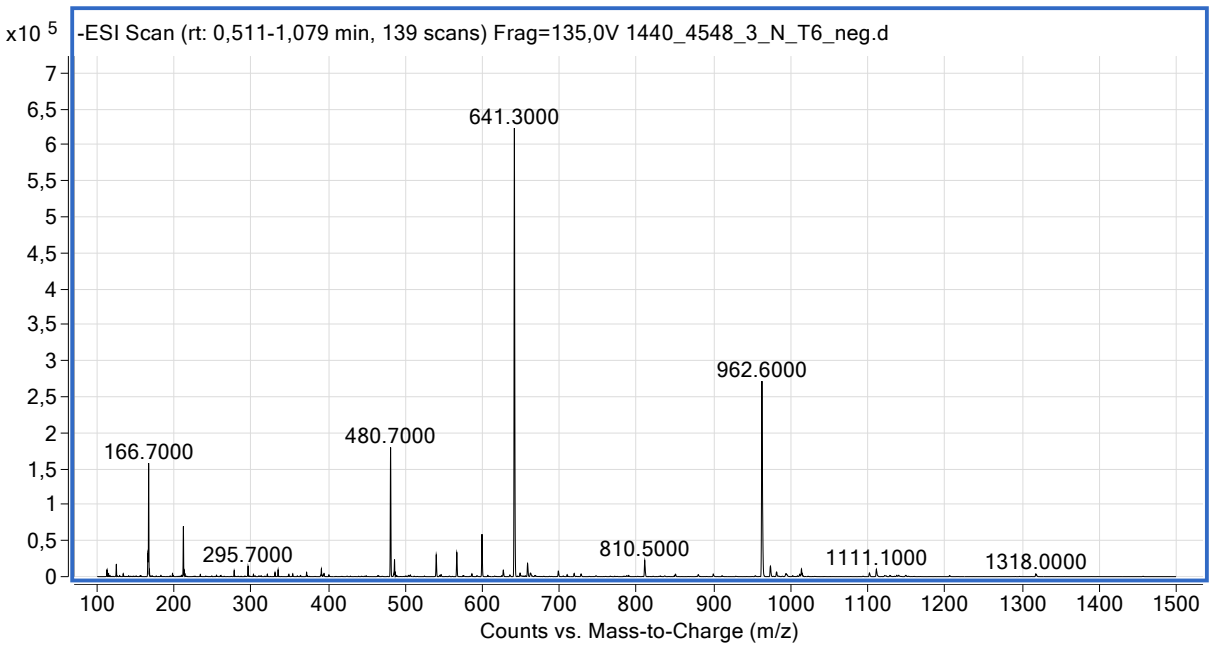

Figure S16. Mass spectrum (ESI LC-MS/MS in negative mode) of 5′-TTTTT^{NPh}T-3′ (3′-NPh-T6, Table 1).

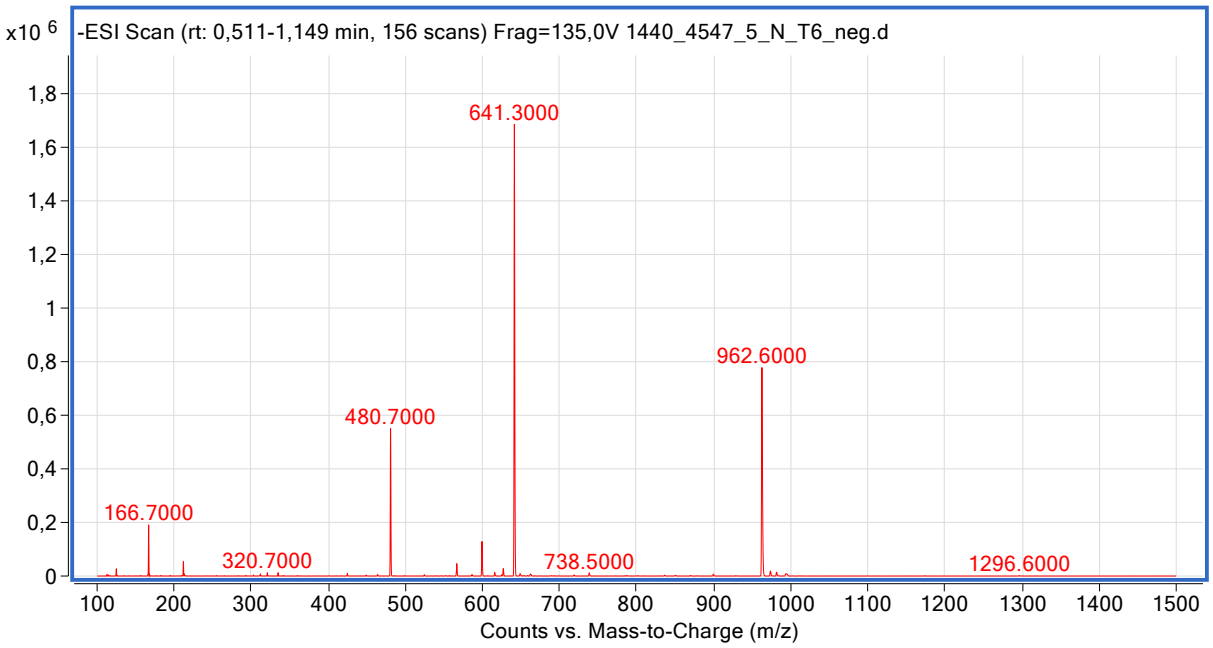

Figure S17. Mass spectrum (ESI LC-MS/MS in negative mode) of 5′-T^{NPh}TTTTT-3′ (5′-NPh-T6, Table 1).

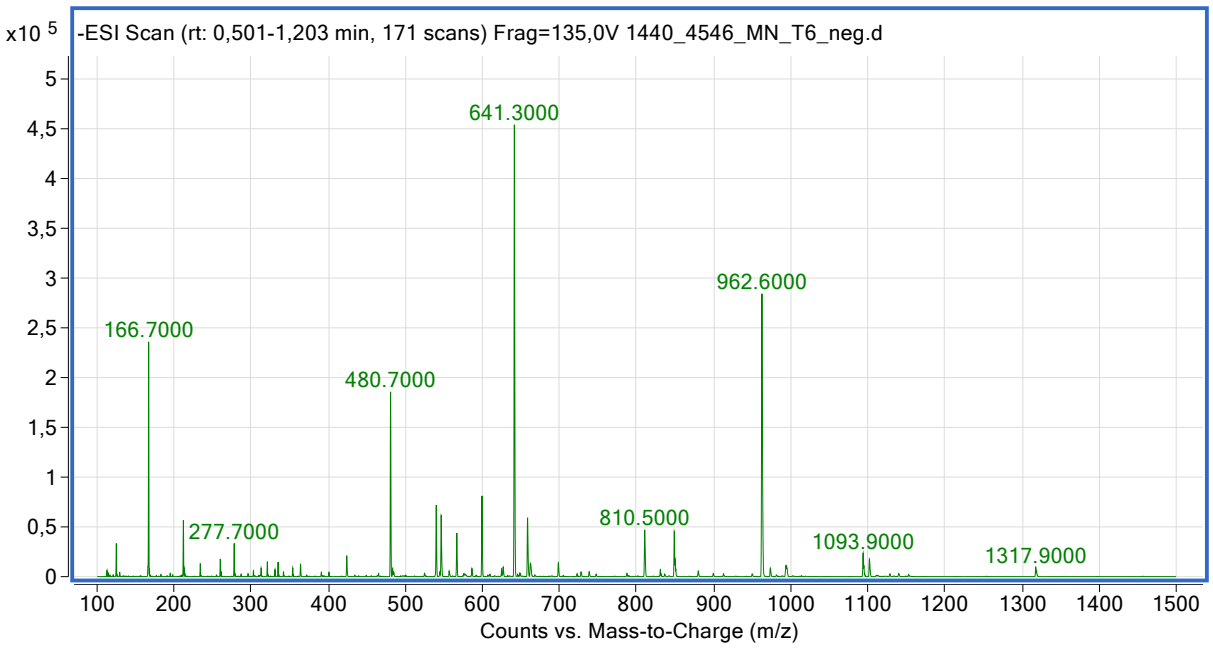

Figure S18. Mass spectrum (ESI LC-MS/MS in negative mode) of 5′-TTT^{NPh}TTT-3′ (M-NPh-T6, Table 1).

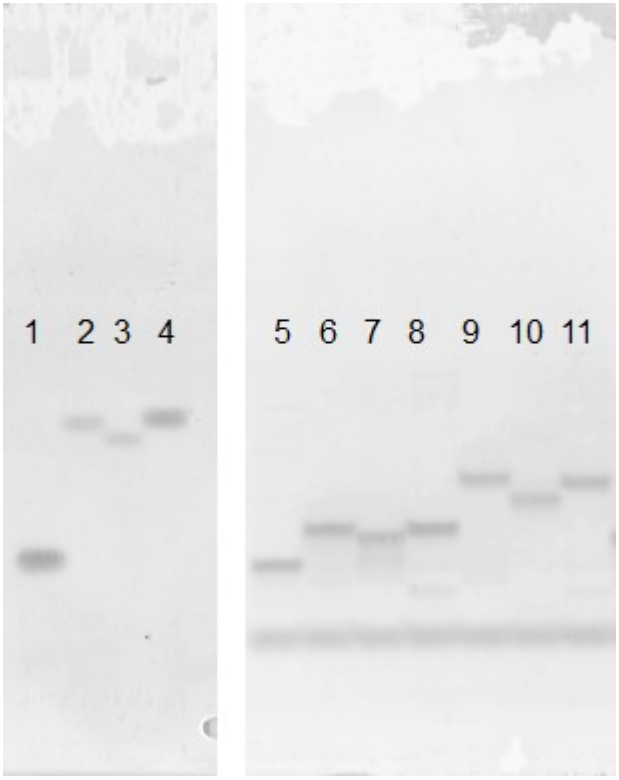

Figure S19. Electrophoretic analysis of the oligonucleotides' reaction mixtures in a denaturing 20 % polyacrylamide gel. Left - hexathymidylate with the *N*-naphthoimidazole group; lanes: 1) 5′-TTTTTT-3′, 2) 5′-TTTTT^{NPh}T-3′, 3) 5′-TTT^{NPh}TTT-3′, and 4) 5′- T^{NPh}TTTTT-3′. Right - decamers with heteronucleotide sequence; lanes: 5) 5′-GCGCCAAACA-3′, 9) 5′-GCGCCAAAC^{NPh}A3′, 10) 5′-GCGCC^{NPh}AAACA-3′, and 11) 5′-G^{NPh}CGCCAAACA-3′. Lanes 6-8 are reaction mixtures of decamers with N-caffeine modification 6) 5′-GCGCCAAAC^{C}A3′, 6) 5′-GCGCC^{C}AAACA-3′, and 8) 5′-G^{C}CGCCAAACA-3′ [A.I. Novgorodtseva, A.Y. Vorob'ev, A.A. Lomzov, S. V. Vasilyeva, Synthesis and physicochemical properties of new phosphoramide oligodeoxyribonucleotides. I. *N*-caffeine derivatives, Bioorg Chem 157 (2025) 108313. https://doi.org/10.1016/J.BIOORG.2025.108313].

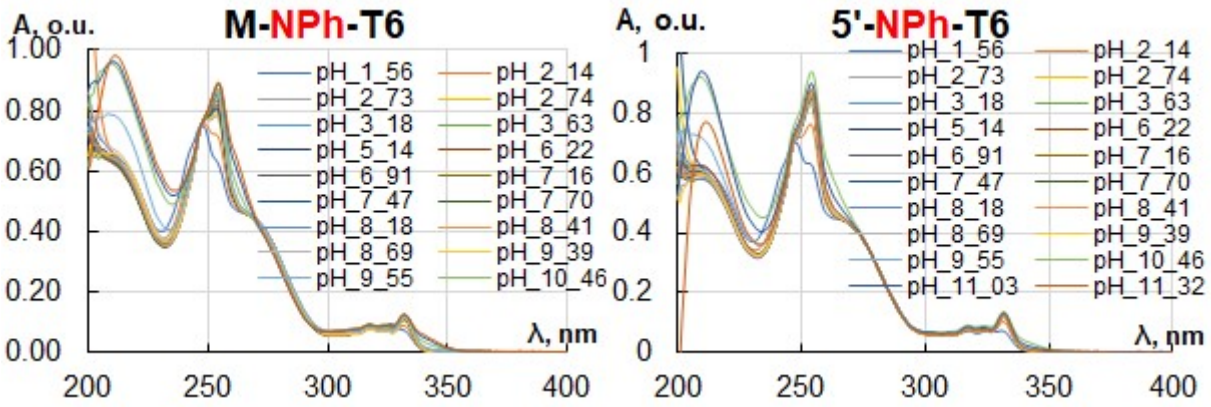

Figure S20. Normalized UV spectra of 5′-TTT^{NPh}TTT-3′ and 5′-T^{NPh}TTTTT-3′ oligonucleotides across a range of pH (C = 1.5 x 10^{-5} M).

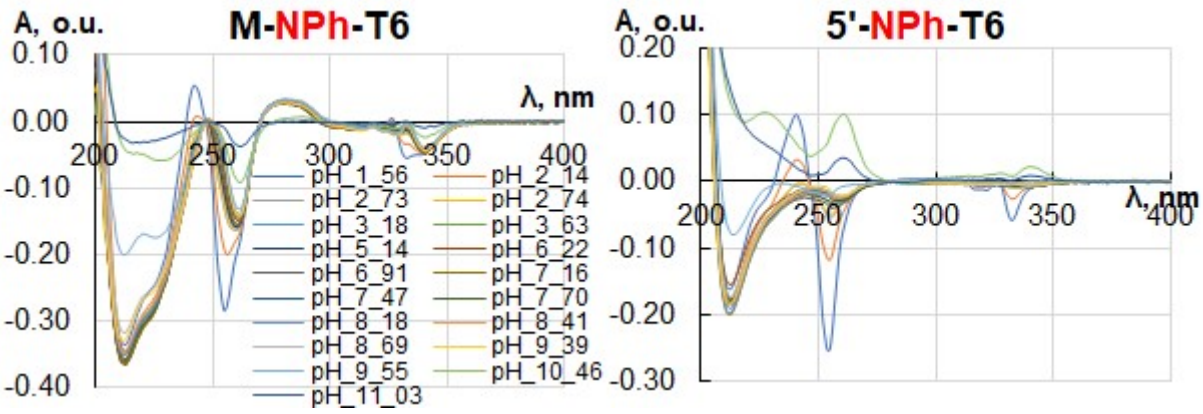

Figure S21. Spectral difference plot of 5′-TTT^{NPh}TTT-3′ and 5′-T^{NPh}TTTTT-3′ oligonucleotides obtained by subtraction of spectra at pH 11.32.

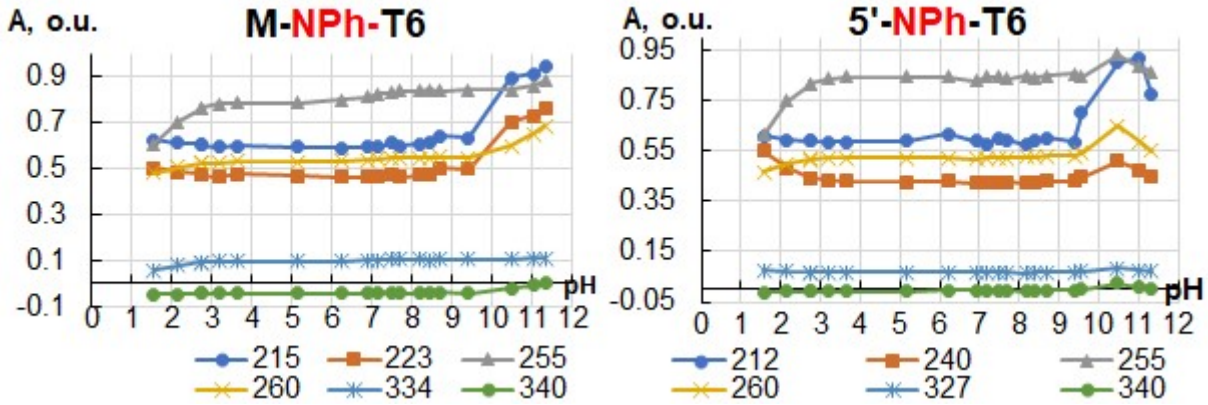

Figure S22. Dependence of the changes in optical density on pH for 5′-T^{NPh}TTTTT-3′ and 5′-TTT^{Nph}TTT-3′ oligonucleotides.

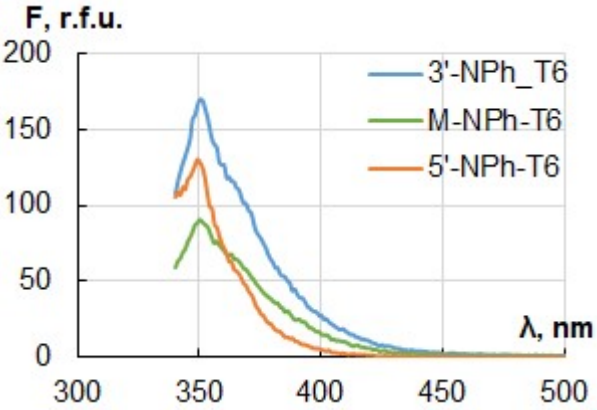

Figure S23. Emission spectra for oligonucleotides 3'-NPh-T6, M-NPh-T6, 5'-NPh-T6 (Table 1) in water, the concentration was 0.1 mM; excitation wavelength 330 nm. R.f.u.: relative fluorescence units.

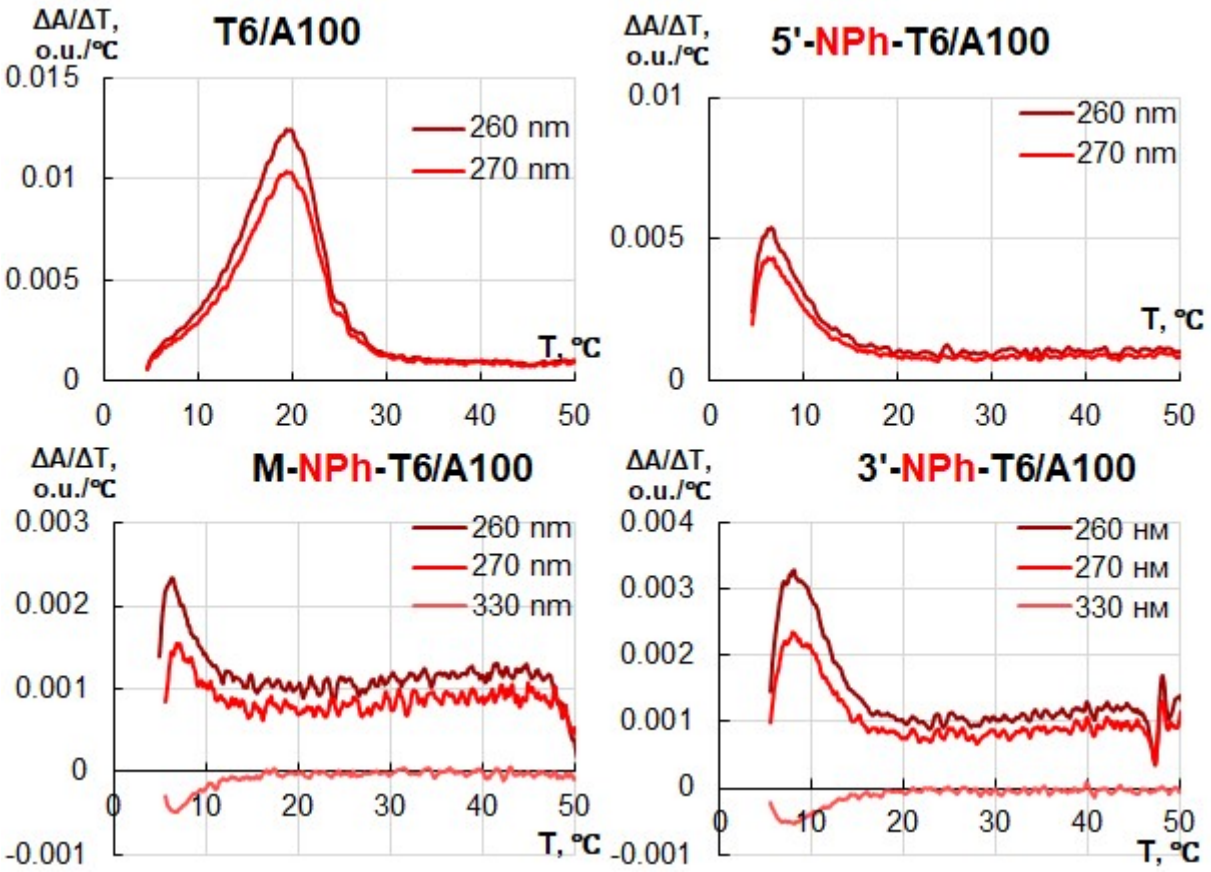

Figure S24. Differential UV melting curves of native and modified hexathymidylate at 260 nm and 270 nm

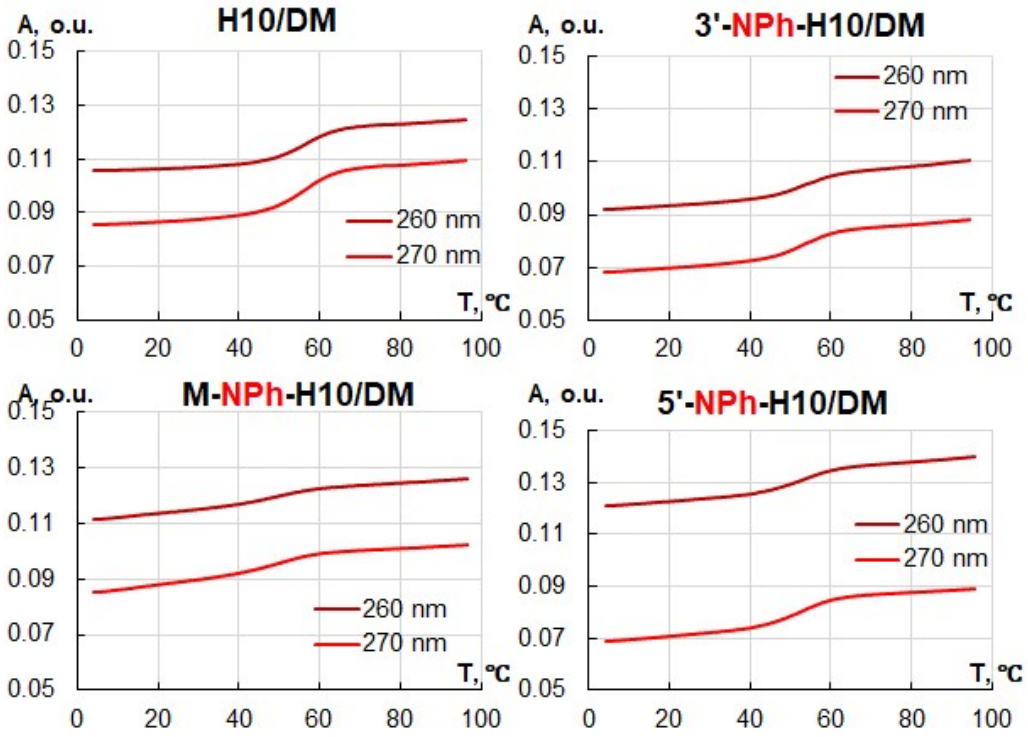

Figure S25. UV melting curves of the decamers with DNA at 260 nm and 270 nm in 1 M NaCl and 10 mM sodium cacodylate, pH 7.2. Total concentration of oligonucleotides is 5 μM.

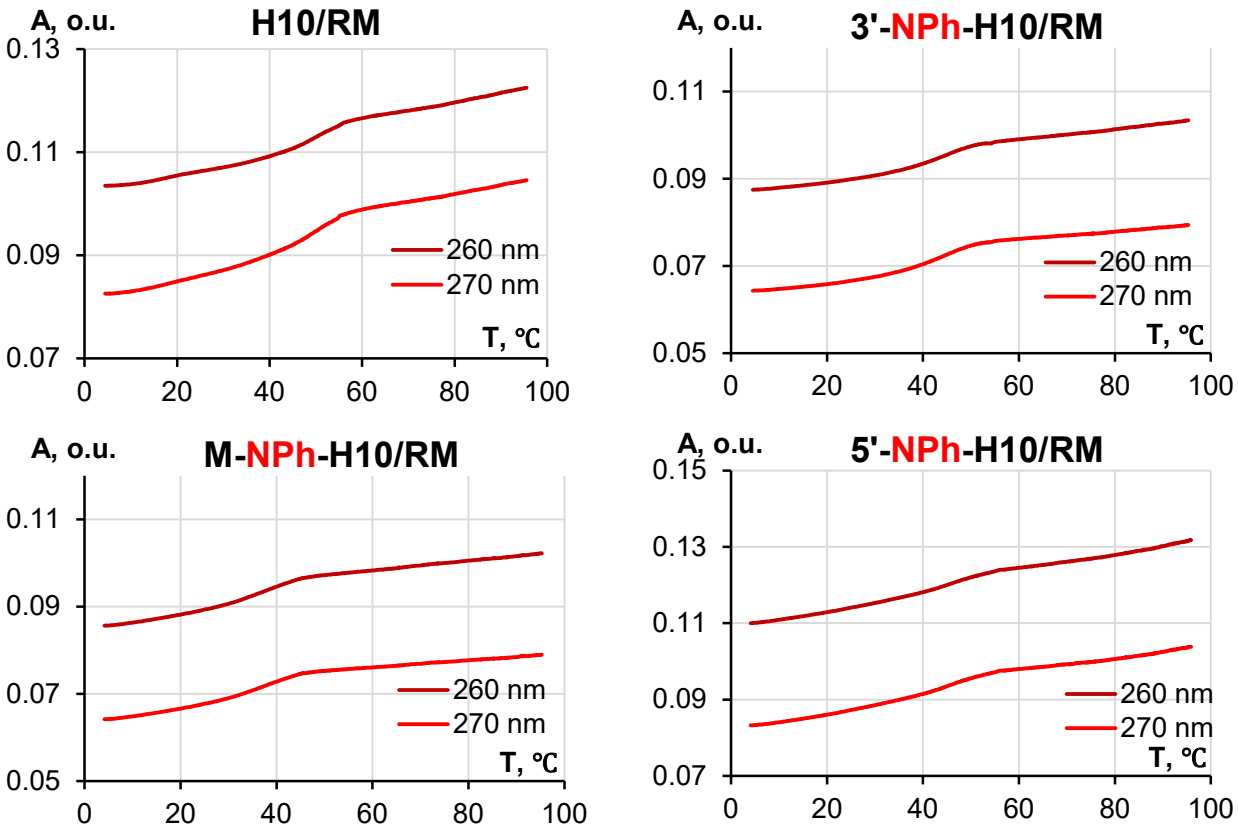

Figure S26. UV melting curves of the decamers with RNA at 260 nm and 270 nm in 1 M NaCl and 10 mM sodium cacodylate, pH 7.2. Total concentration of oligonucleotides is 10 μM.

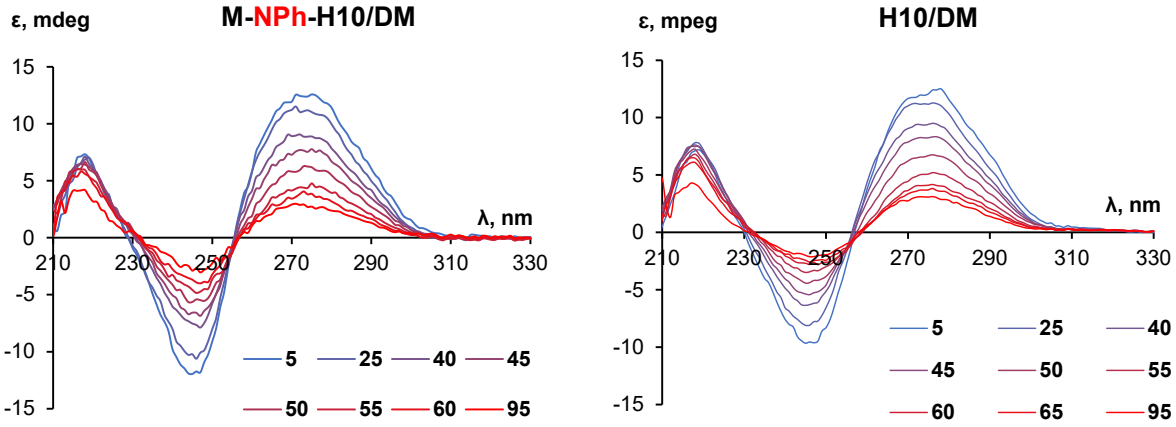

Figure S27. Temperature dependence of CD spectra of the complexes in the range 5–95°C in 1 M NaCl and 10 mM sodium cacodylate, pH 7.2. Total concentration of oligonucleotides is 10 μM.

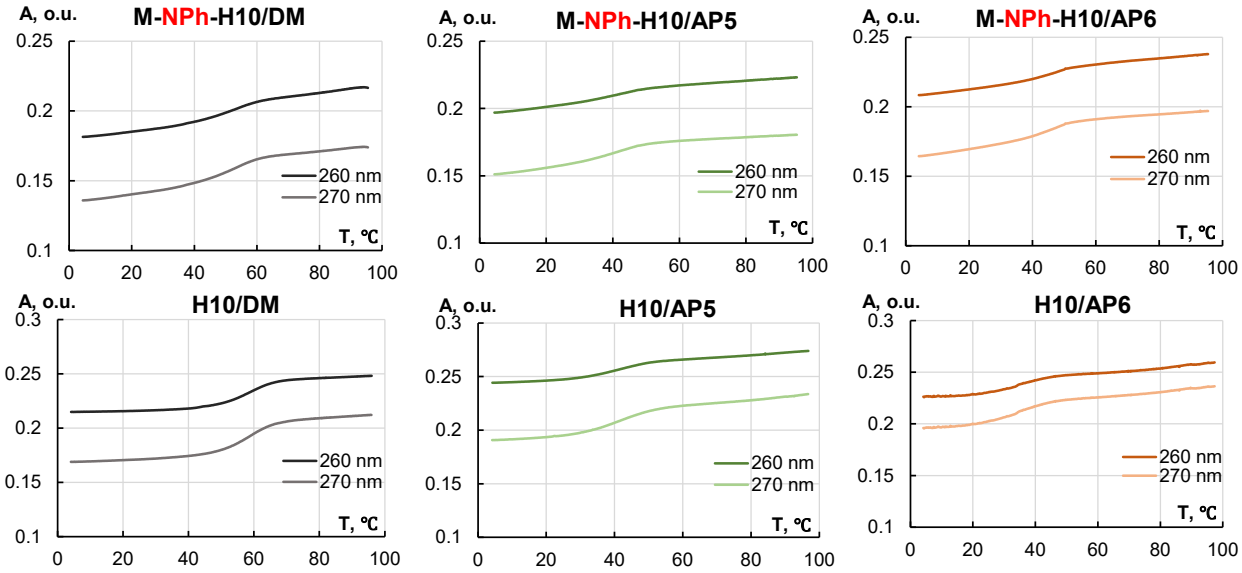

Figure S28. UV melting curves of the decamers with DNA at 260 nm and 270 nm in 1 M NaCl and 10 mM sodium cacodylate, pH 7.2. Total concentration of oligonucleotides is 5 μM.

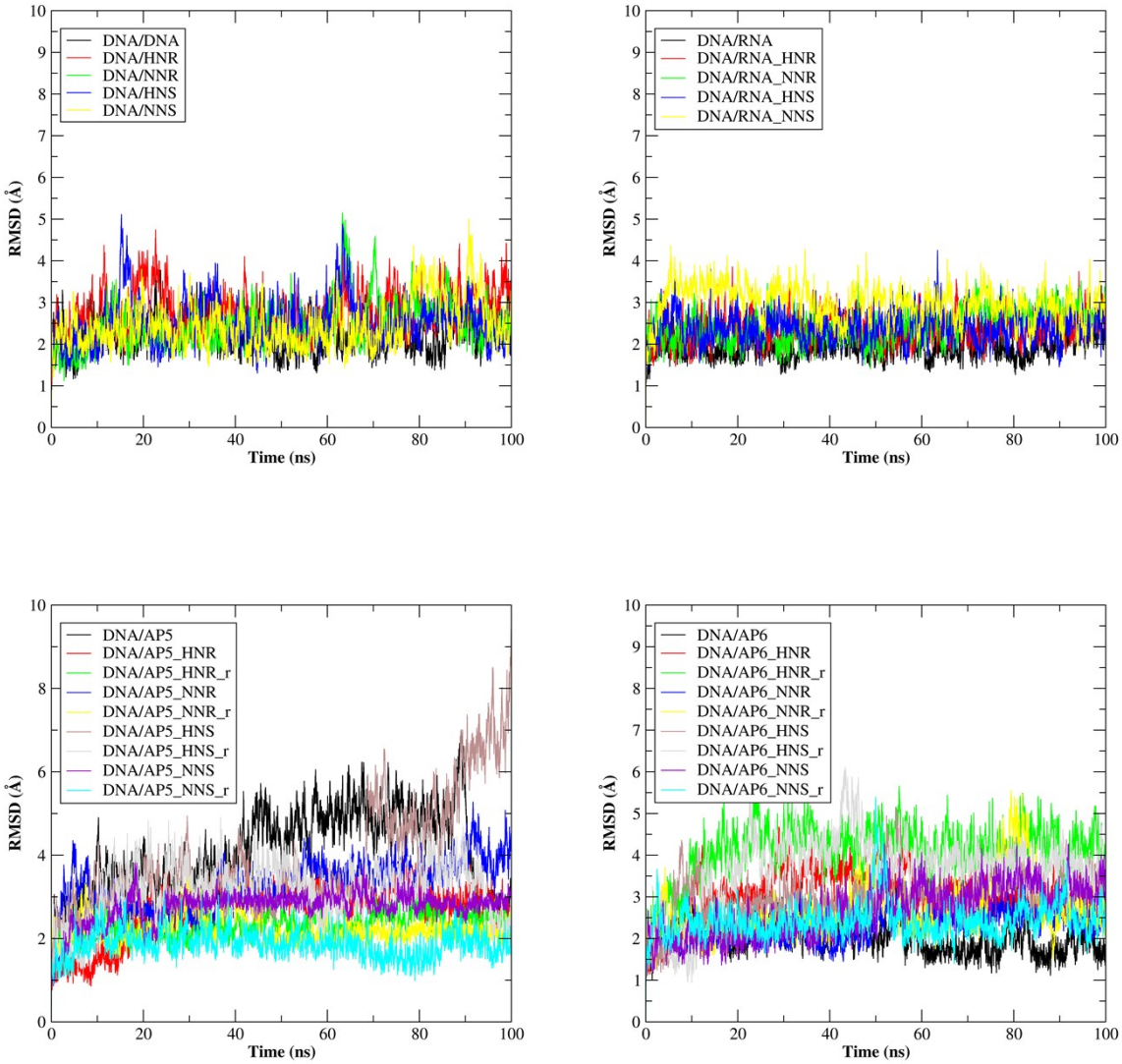

Figure S29. Time-dependent root mean square deviation of native and modified complexes with NPh modification in protonated (HN) and deprotonated (NN) state of Rp or Sp diastereomer. The first structure in each trajectory was used as the reference structure in the RMSD calculation.

Table S1. Structural analysis of complexes containing the NPh modification in protonated (HN) and deprotonated (NN) states of the Rp or Sp diastereomers. RMSD values were calculated for the most representative structures from the MD trajectory of modified complexes relative to the native structure, considering only heavy atoms of the nucleobases and the sugar-phosphate backbone. Structural Features describe the location of the modification and other characteristics of the most representative structures in the MD trajectory.

Complex	Modifi-cation	RMSD, Å	**Structural Features**
DNA/DNA	HNR	1.596	Modification is located externally, forming a hydrogen bond with O3′
	NNR	1.261	Modification is located externally, forming a hydrogen bond with O3′
	HNS	1.26	Modification is located externally, forming a hydrogen bond with O5′
	NNS	1.172	Modification is located externally, forming a hydrogen bond with O5′
DNA/RNA	HNR	0.831	Modification is located externally, forming a hydrogen bond with O3′
	NNR	2.154	Modification is located externally, forming a hydrogen bond with O3′
	HNS	0.869	Modification is located externally, forming a hydrogen bond with O5′
	NNS	0.989	Modification is located externally, forming a hydrogen bond with O5′
AP5	HNR	7.16	Modification is located in the minor groove
	HNR_r	4.927	Modification is located in the minor groove; adenine is flipped out of the double helix
	NNR	4.937	Modification is located externally, forming a hydrogen bond with O3′
	NNR_r	4.225	Modification is located in the minor groove, coplanar with the base pair
	HNS	5.333	Modification is located in the major groove
	HNS_r	5.189	Modification is intercalated into the double helix
	NNS	5.081	Modification is located outside the double helix, in stacking with adenine
	NNS_r	4.162	Modification is intercalated into the double helix
AP6	HNR	3.053	Modification is positioned in the minor groove
	HNR_r	4.007	Modification is intercalated into the double helix
	NNR	3.615	Modification is located in the minor groove
	NNR_r	3.99	Modification is intercalated into the double helix
	HNS	3.327	Modification is located externally, forming a hydrogen bond with O5′
	HNS_r	3.264	Modification is intercalated into the double helix
	NNS	2.606	Modification is located in the major groove
	NNS_r	3.867	Modification is intercalated into the double helix

Table S2. Analysis of the MMGBSA energies of complexes containing the NPh modification in protonated (HN) and deprotonated (NN) states of the Rp or Sp diastereomers

Complex	Modification	E (MMGBSA), kcal/mol	E(native)-E(NPh), kcal/mol
DNA/DNA	native	-97.3	
	HNR	-100.6	3.2
	NNR	-100.1	2.8
	HNS	-100.7	3.4
	NNS	-99.9	2.5
DNA/RNA	native	-96.3	
	HNR	-99.2	2.9
	NNR	-98.6	2.2
	HNS	-99.5	3.1
	NNS	-94.7	-1.6
AP5	native	-95.3	-2.0*
	HNR	-117.4	22.1
	HNR_r	-102.7	7.4
	NNR	-96.0	0.7
	NNR_r	-96.5	1.2
	HNS	-86.1	-9.2
	HNS_r	-101.2	5.9
	NNS	-96.2	0.9
	NNS_r	-107.2	11.9
AP6	native	-90.9	-6.5*
	HNR	-107.9	17.1
	HNR_r	-97.7	6.8
	NNR	-101.6	10.7
	NNR_r	-94.0	3.1
	HNS	-89.4	-1.5
	HNS_r	-97.8	7.0
	NNS	-95.2	4.3
	NNS_r	-91.0	0.2

* Values calculated relative native DNA/DNA duplex without lesion.